NEOPLASIA
www.neoplasia.com

Volume 23 Number 1 Month 2021 pp. 58–67 58

Original Research

Tumor treating fields (TTFields) impairs aberrant glycolysis in glioblastoma as evaluated by [18F]DASA-23, a non-invasive probe of pyruvate kinase M2 (PKM2) expression ☆, ☆☆

Chirag B. Patel [a,b,2,*]; Corinne Beinat [a,2]; Yuanyang Xie [a,1]; Edwin Chang [a]; Sanjiv S. Gambhir [a,c]

[a] Molecular Imaging Program at Stanford (MIPS), Department of Radiology, Stanford University School of Medicine, Stanford, CA, USA
[b] Division of Adult Neuro-Oncology, Department of Neurology and Neurological Sciences, Stanford University School of Medicine, Stanford, CA, USA
[c] Departments of Bioengineering and Materials Science & Engineering, Stanford University, Stanford, CA, USA

Abstract

Despite the anti-proliferative and survival benefits from tumor treating fields (TTFields) in human glioblastoma (hGBM), little is known about the effects of this form of alternating electric fields therapy on the aberrant glycolysis of hGBM. [18F]FDG is the most common radiotracer in cancer metabolic imaging, but its utility in hGBM is impaired due to high glucose uptake in normal brain tissue. With TTFields, radiochemistry, Western blot, and immunofluorescence microscopy, we identified pyruvate kinase M2 (PKM2) as a biomarker of hGBM response to therapeutic TTFields. We used [18F]DASA-23, a novel radiotracer that measures PKM2 expression and which has been shown to be safe in humans, to detect a shift away from hGBM aberrant glycolysis in response to TTFields. Compared to unexposed hGBM, [18F]DASA-23 uptake was reduced in hGBM exposed to TTFields (53%, $P < 0.05$) or temozolomide chemotherapy (33%, $P > 0.05$) for 3 d. A 6-d TTFields exposure resulted in a 31% reduction ($P = 0.043$) in 60-min uptake of [18F]DASA-23. [18F]DASA-23 was retained after a 10 but not 30-min wash-out period. Compared to [18F]FDG, [18F]DASA-23 demonstrated a 4- to 9-fold greater uptake, implying an improved tumor-to-background ratio. Furthermore, compared to no-TTFields exposure, a 6-d TTFields exposure caused a 35% reduction in [18F]DASA-23 30-min uptake compared to only an 8% reduction in [18F]FDG 30-min uptake. Quantitative Western blot analysis and qualitative immunofluorescence for PKM2 confirmed the TTFields-induced reduction in PKM2 expression. This is the first study to demonstrate that TTFields impairs hGBM aberrant glycolytic metabolism through reduced PKM2 expression, which can be non-invasively detected by the [18F]DASA-23 radiotracer.

Neoplasia (2021) 23, 58–67

Keywords: Tumor treating fields (TTFields), Glioblastoma, Pyruvate kinase M2 (PKM2), Tumor glycolysis, Warburg effect

Abbreviations: [18F]DASA-23, 1-((2-fluoro-6-[18F]fluorophenyl)sulfonyl)-4-((4-methoxyphenyl)sulfonyl)piperazine; [18F]FDG, 2-deoxy-2-[18F]fluoro-D-glucose; ATP, adenosine triphosphate; BSA, bovine serum albumin; DAPI, 4′,6-diamidino-2-phenylindole; DPBS, Dulbecco's phosphate buffered saline; FBS, fetal bovine serum; GAPDH, glyceraldehyde 3-phosphate dehydrogenase; GBM, glioblastoma; GBM39, human glioblastoma cell line, courtesy of Dr. Paul Mischel (University of California at San Diego); MGMT, O^6-methylguanine-DNA-methyltransferase; MRI, magnetic resonance imaging; PBS, phosphate buffered saline; PET, positron emission tomography; PK, pyruvate kinase; PKM2, pyruvate kinase M2; RT, room temperature; TTFields, tumor treating fields; TMZ, temozolomide; U87, human glioblastoma cell line.

* Corresponding author.
E-mail address: cbpatel@stanford.edu (C.B. Patel).

☆ Declaration of interests: The authors declare the following financial interests/personal relationships which may be considered as potential competing interests: • CBP: Patent application with Novocure, Ltd. • CB: Patent application with Novocure, Ltd. • YX: None. • EC: Patent application with Novocure, Ltd.; honorarium and grant from Novocure, Ltd. • SSG: Patent application with Novocure, Ltd.; grant from Novocure, Ltd.

☆☆ Funding sources: None of the funding sources had involvement in study design, data collection/analysis/interpretation, writing of the report, or decision to submit the article for publication. Ben and Catherine Ivy Foundation (to SSG) · Novocure, Ltd. (to SSG and EC) · Stanford-Asia Medical Fund C.J. Huang Medical Fellowship (to YX) · Stanford Cancer Institute Fellowship Award for Cancer Research (to CBP) · Stanford School of Medicine Translational Research and Applied Medicine Fellowship (to CB)

[1] Present address: Department of Neurosurgery, Central South University Xiangya School of Medicine, Changsha, Hunan Province, CHINA.

[2] Equal contribution.

Received 8 August 2020; received in revised form 2 November 2020; accepted 3 November 2020

© 2020 The Authors. Published by Elsevier Inc. This is an open access article under the CC BY-NC-ND license (http://creativecommons.org/licenses/by-nc-nd/4.0/)

https://doi.org/10.1016/j.neo.2020.11.003

Introduction

Tumor treating fields (TTFields) is emerging as the fourth therapeutic modality after standard-of-care surgical resection, radiation, and temozolomide (TMZ) chemotherapy for the treatment of glioblastoma (GBM) [1-4]. TTFields is alternating electric fields in the 100 to 500 kHz frequency range delivered to tumors via transmitting electrodes placed on the skin [5]. In a phase III clinical trial of patients with newly-diagnosed GBM, combining 200 kHz TTFields with maintenance adjuvant TMZ prolonged overall survival from 16 to 21 mo and increased the 5-y survival rate from 5% to 13% [6,7], compared to maintenance adjuvant TMZ alone. In addition to FDA approval in newly-diagnosed and recurrent GBM, TTFields has been approved for use in patients with pleural malignant mesothelioma and clinical trials in other solid organ cancers are underway.

TTFields has been shown to interfere with mitosis in rapidly dividing cancer cells, thereby impairing cancer proliferation [8,9]. We have recently shown that TTFields increases the permeability of the GBM cell membrane [10]. Yet, the effect of TTFields on cancer metabolism is not well understood. A limited number of clinical studies have evaluated the effects of TTFields on GBM physiology. Two reports demonstrated that TTFields results in a decreased uptake of amino acid-based positron emission tomography (PET) radiotracers [11,12], indicating an impairment of amino acid metabolism. Using perfusion and spectroscopic magnetic resonance imaging (MRI), a separate study identified a reduction in maximum relative cerebral blood volume and choline/creatinine ratio over time in patients with GBM on combination TTFields and TMZ chemotherapy [13].

To survive conditions of rapid cell division, tumor cells undergo metabolic reprogramming. The idea of metabolic modulation was first reported almost a century ago by Otto Warbug, following the observation that cancer cells demonstrated the increased consumption of glucose and production of lactate relative to normal tissue, even under conditions of abundant oxygen [14]. This effect, known as the Warburg effect, has been extensively exploited clinically with 2-deoxy-2-[^{18}F]fluoro-D-glucose ([^{18}F]FDG), a radiotracer that has been successful in the identification and characterization of primary and metastatic cancers during initial staging and response assessment [15]. However, the role of [^{18}F]FDG PET is limited in brain tumors due to the elevated background signal from glucose metabolism in the healthy brain, making it difficult to distinguish brain tumors from normal brain with [^{18}F]FDG PET imaging [16].

We have recently developed [^{18}F]DASA-23, a radiotracer that provides a measure of the expression of pyruvate kinase M2 (PKM2) [17], to overcome the limitations of [^{18}F]FDG for the molecular imaging of brain tumors. PK catalyzes the final step in glycolysis, converting phosphoenolpyruvate to pyruvate and yielding adenosine triphosphate [18]. Reduced PK activity results in a diminished production of pyruvate, therefore enabling the accumulation of upstream glycolytic intermediates and shifting metabolism towards the anabolic phase [19]. Cancer cells exploit this effect by primarily utilizing the PKM2 isoform of PK, whose activity can be dynamically controlled between the less active PKM2 dimer and the highly active PKM2 tetramer [20]. PKM2 is found in most cells with the exception of adult muscle, brain and liver, and is preferentially expressed in all cancers [21]. PKM2 expression in primary brain tumors is well established. Whereas grade I to III gliomas exhibit modestly increased levels of PKM2 RNA and protein expression relative to normal brain tissue, GBM displays a further 3- to 5-fold increase in PKM2 RNA and protein expression compared to even grade III gliomas [22].

PKM2 expression is associated with the enhanced uptake of glucose, increased production of lactate, and a reduction in oxygen consumption; these effects are reversed by genetic modifications to replace PKM2 expression with PKM1 [20,23]. PKM2 is therefore a key regulator of the Warburg effect, the elevated levels of dimeric PKM2 in cancer cells contributes to anabolic glucose metabolism, supporting rapid cell proliferation and ultimately benefiting cancer cell proliferation and growth [23].

The effects of TTFields on cancer cell proliferation have been well-studied but it remains unclear whether changes in other key aspects of cancer cell function are also affected by TTFields. TTFields likely targets cancer in a myriad of ways and perturbs a multitude of individual proteins and molecular pathways [9,24-29]. However, the effects of TTFields on GBM metabolism is not well understood. Here, we report the effects of TTFields on GBM cell aberrant glycolysis as measured by [^{18}F]DASA-23 and [^{18}F]FDG.

Materials and methods

Cell lines and culture media

Human GBM U87 cells were purchased from ATCC (Manassas, VA) and GBM39 cells were received as a gift from Dr. Paul Mischel (Ludwig Institute for Cancer Research, University of California, San Diego). Identity of cell lines was confirmed by the source. Cells were studied in DMEM (Gibco, Gaithersburg, MD) containing 10% fetal bovine serum (Gibco), and 1 × antibiotic/antimycotic (Gibco).

IC_{50} determination in U87 cells

TMZ was purchased from MedChemExpress (Monmouth Junction, NJ). The IC_{50} of TMZ was determined using a 72 h incubation period in U87 cells. In brief, U87 cells were plated in a 96-well plate (5×10^3 cells per well, $n = 3$ per condition) and after 24 h, exposed to serial dilutions of TMZ stock (100 mM in dimethyl sulfoxide (DMSO)) which ranged from 33 mM to 14 μM. DMSO vehicle was used for control wells. After 72 h, the Presto Blue Viability Assay (Thermo Fisher Scientific Inc., Waltham, MA) was performed and the IC_{50} determined as a function of percent inhibition with respect to DMSO.

TTFields cell culture experiments

Under sterile condition, 22-mm Thermanox Plastic Coverslips (NUNCTM, Rochester, NY) were placed in the center of the wells of 6-well plates. Human GBM cells were seeded onto the center of the coverslips at a concentration of 50,000 cells/200 μL or 10,000 cells/200 μL for 3- and 6-d experiments, respectively (see Table 1 and Figure 1).

TTFields cell culture experiments (continued)

Six-well plates were carefully transferred into a standard humidified incubator (37 ˚C, 5% CO_2). At least 6 coverslips were seeded per cell line per TTFields treatment duration. 24 h later, after sufficient time for the cells to adhere to the coverslips, 2 mL of pre-warmed culture media was carefully added to each well of the 6-well plates. 24-h later, half of the coverslips of each cell line were transferred to the ceramic dishes of the inovitro TTFields system (Novocure, Ltd. Haifa, Israel). Two milliliter of pre-warmed culture media was added to the ceramic dishes. Ceramic dishes were attached to the inovitro base plates and placed in a cooled incubator (20 ˚C setpoint, 5% CO_2). A local temperature of 37 ˚C was maintained in each ceramic dish by the inovitro system. TTFields was delivered at 200 kHz; the ambient temperature achieved in the incubator during the experiments was 24 ˚C, corresponding to a TTFields field strength of 3.2 V/cm (peak-peak). and 1 to 4 V/cm. For the control group, at least 3 coverslips were seeded per cell line in 6-well plates and transferred to a standard humidified incubator (37 ˚C, 5% CO_2). Each day during the TTFields experiment, the media was exchanged for fresh pre-warmed media for both TTFields and control groups. After each experiment, the TTFields and control coverslips were used for radiotracer uptake studies or transferred to 6-well plates for immunofluorescence studies. Coverslips

Table 1

Timeline for 3- and 6-d tumor treating fields (TTFields) experiments.

Day	Steps for 3-d TTFields experiment	Steps for 6-d TTFields experiment
1		Seed cells onto center of coverslips (10,000 cells/200 µL media per coverslip) in 6-well plates
2		Add 2 mL culture media to each well
3		Transfer TTFields coverslips into ceramic dishes of inovitro system, attach to base plates, begin experiment. For control coverslips, maintain in regular incubator (37 °C, 5% CO_2, 95% room air)
4	Seed cells onto center of coverslips (50,000/200 µL media per coverslip) in 6-well plates	Exchange coverslip media for fresh media in both groups
5	Add 2 mL culture media to each well	Exchange coverslip media for fresh media in both groups
6	Transfer TTFields coverslips into ceramic dishes of inovitro system, attach to base plates, begin experiment. For control coverslips, maintain in regular incubator (37 °C, 5% CO_2, 95% room air)	Exchange coverslip media for fresh media in both groups
7	Exchange coverslip media for fresh media in both groups	Exchange coverslip media for fresh media in both groups
8	Exchange coverslip media for fresh media in both groups	Exchange coverslip media for fresh media in both groups
9	End experiment. Wash all coverslips (both groups) in HBSS, dry, and evaluate for [^{18}F]DASA-23 uptake	End experiment. Wash all coverslips (both groups) in HBSS, dry, and evaluate for [^{18}F]DASA-23 uptake

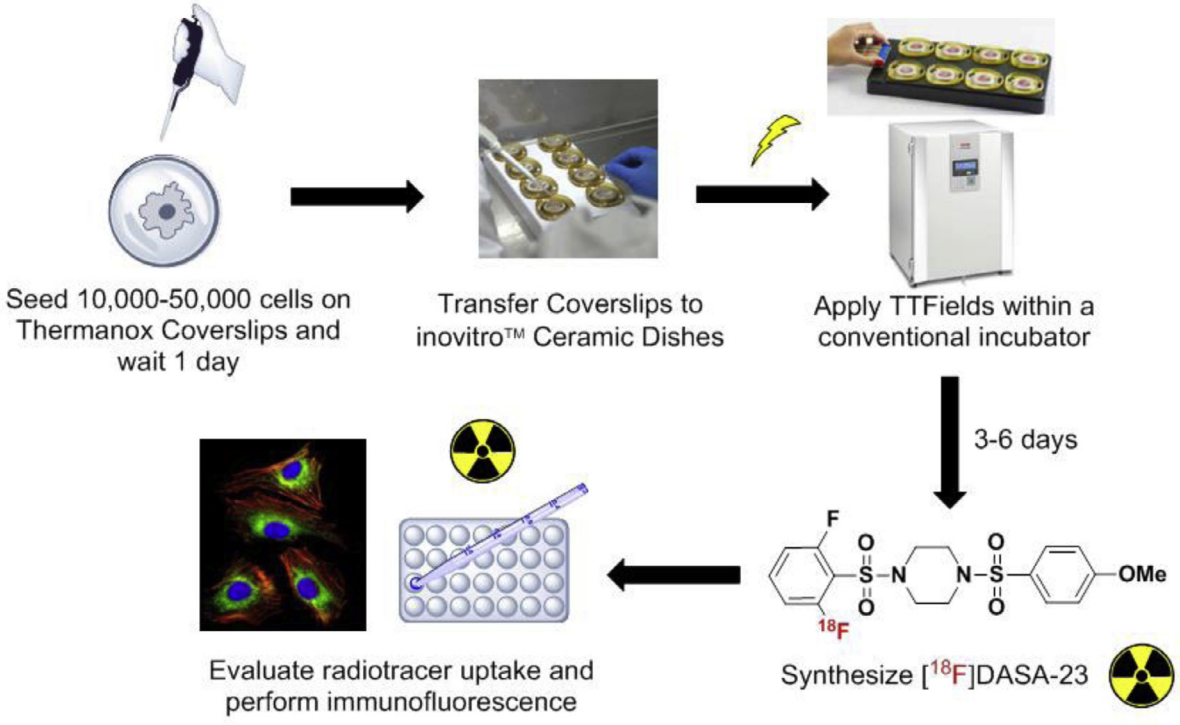

Figure 1. Schematic of TTFields experiments and radiotracer uptake studies. 10,000 to 50,000 single cells were suspended in 200 µL media and seeded into the center of a 22 mm diameter cover slip. Cells were allowed to adhere overnight in a conventional tissue culture incubator. Subsequently, an additional 2 mL of media was added to each well and the coverslips maintained in a conventional incubator for an additional day. Coverslips were then transferred to the wells of an inovitro TTFields ceramic dish system (Novocure, Ltd.) and then connected in base plates that were connected to the power box of the inovitro system for the delivery of alternating electric fields. Control cell coverslips were maintained in a conventional tissue culture incubator. Cells were grown for the appropriate period of time (3- or 6 d) with daily changes of media. At the appropriate time point, [^{18}F]DASA-23 was synthesized, and the radiotracer uptake evaluated.

were washed twice with PBS and then fixed for 30 min at room temperature with 4% paraformaldehyde (w/v) in PBS. They were then washed twice with PBS and stored in wash buffer (0.1% BSA [w/v] in Dulbecco's phosphate buffered saline (DPBS) [Thermo Fisher Scientific, Waltham, MA]) at 4 °C.

Radiochemistry

[^{18}F]FDG was obtained from routine production at the Stanford University Cyclotron and Radiochemistry Facility. [^{18}F]DASA-23 was produced according to previously described methods [17]. In brief, [^{18}F]F (no carrier added) in [18O] water was trapped on a PS-HCO3 cartridge and eluted with 1 mL of a solution containing Kryptofix222 (15 mg) and K2CO3 (3.5 mg) in 9:1 acetonitrile/water. The K222/K[^{18}F]F complex was dried under a stream of helium at 65 °C for 3 min, followed by further heating at 85 °C for 1 min. After cooling to 40 °C, DASA-23 nitro precursor (~350 µg) in 1 mL of DMF was added to the reactor, and the solution was heated to 110 °C for 20 min. The reaction mixture was then diluted with water (8 mL) and passed through a C18 cartridge, the radiolabeled product was eluted with acetonitrile (1.5 mL) and water (2.0 mL) into a pre-HPLC vial for subsequent purification. The crude solution was injected onto a Gemini C18 semi-preparative reverse-phase column and desired HPLC fraction (retention time ~18 min) containing the radiolabeled product was collected in a flask pre-filled with water (20 mL). The diluted product was passed then trapped on a C18 cartridge and rinsed with water (10 mL). The final product was eluted with ethanol (1 mL) and saline (9 mL). Radiochemical yield was 2.61% ± 1.54% (non-decay corrected at end of synthesis) with a specific activity of 2.59 ± 0.44Ci/µmol ($n = 10$) and radiochemical and chemical purity greater than 95%.

Radiotracer uptake and retention studies

For uptake studies, pre-warmed DMEM was used for [^{18}F]DASA-23 experiments and pre-warmed HBSS (Thermo Fisher Scientific, Waltham, MA) was used for experiments involving [^{18}F]FDG. After 6 d of non-exposure or exposure to TTFields, the culture media around the coverslips containing cells was carefully removed, and 5 µCi of the appropriate radiotracer in either 2 mL of DMEM or HBSS was added per coverslip. Cells were incubated with the specified radiotracer at 37 °C and 5% CO_2 in the presence or absence of TTFields for an additional 30- or 60 min. At 30- and 60 min post-addition of radioactivity, the incubation was halted by removing radiotracer-containing media and placing the plates (containing cells on coverslips) on ice to halt any residual uptake. Coverslips were then washed with ice-cold PBS (3 × 1 mL) and the cells lysed in 1 mL of radioimmunoprecipitation assay buffer (Thermo Fisher Scientific Inc.). A portion of the cell lysates (500 µL) was used to determine the amount of decay-corrected radioactivity on a Cobra II Auto-Gamma Counter (Packard Biosciences Co., Meriden, CT). The remaining cell lysate was used after radioactive decay for determination of protein concentration using a bicinchoninic acid assay (Thermo Fisher Scientific Inc.). Radiotracer uptake values were determined as percentage uptake by additionally counting a proportion of the total radioactivity added to coverslips for each radiotracer.

For the [^{18}F]DASA-23 retention studies, a similar procedure was performed as described above. In one group, cells were not exposed to TTFields for 6 d, followed by a 30-min [^{18}F]DASA-23 uptake period in the continued absence of TTFields. In another group, cells were exposed to TTFields for 6 d, followed by a 30-min [^{18}F]DASA-23 uptake period in the continued presence of TTFields. For both TTFields unexposed and exposed conditions, after the 30-min [^{18}F]DASA-23 uptake period, the retention studies were performed. [^{18}F]DASA-23 was removed from the cell media and replaced with pre-warmed fresh media. The cells underwent either continued TTFields non-exposure or exposure, and at 10- and 30-min later, the amount of [^{18}F]DASA-23 radiotracer retained in the cells (with the remaining [^{18}F]DASA-23 having effluxed out of the cells into the freshly replaced media) was calculated.

PKM2 immunofluorescence

The coverslips with U87 cells were acclimated to room temperature (RT) and washed twice with PBS. Then they were permeabilized with 0.1% TritonX-100 (v/v, Acros Organics, Fair Lawn, NJ) in PBS. They were then washed with DPBS (3 × 5 min). The coverslips were blocked for 1 h at RT in 10% (v/v) fetal bovine serum in DPBS. The blocking solution was then aspirated and the coverslips were washed with wash buffer (2 × 5 min). A monoclonal rabbit antibody was used as the primary antibody for PKM2 detection (Cell Signaling Technology, Danvers, MA). After testing serial dilutions of the antibodies, the primary antibody was diluted 1:500 in 3% BSA (v/v) in DPBS, applied to the coverslips and incubated at 4 °C overnight. The next day, the coverslips were washed with DPBS (3 × 5 min). They were subsequently incubated at room temperature, protected from light, with the fluorophore-conjugated anti-rabbit secondary antibody (Cell Signaling Technology) diluted 1:1000 in 10% FBS (v/v) in DPBS for 1 h. The secondary antibody was then aspirated and the coverslips were washed with DPBS (3 × 5 min) in the dark. The coverslips were air dried and mounted to Superfrost Plus microscope slides (Fisher Scientific Inc.) using Vectashield Antifade Mounting Medium with DAPI (Vector Laboratories, Burlingame, CA). The edges of the coverslips were sealed with clear nail varnish. The coverslips were imaged on a NanoZoomer 2.0-RS whole slide imager (Hamamatsu, Hamamatsu City, Japan) at 20 × magnification and images were exported as TIFF files for qualitative comparison.

Western blotting

At the completion of studies, cells grown on coverslips were lysed in non-ionic detergent (% RIPA lysis and extraction buffer [Thermo Fisher Scientific, Inc., Waltham, MA]) supplemented with Halte Protease Inhibitor Cocktail (Thermo Fisher Scientific Inc.) and stored at -80 °C until further processing. PKM2 monoclonal rabbit antibody (1:3000 dilution, Cell Signaling Technology) was used in a standard Western blotting protocol according to the manufacturer's instructions. Rabbit anti-GAPDH antibody (1:5000 dilution, Cell Signaling Technology) was used as loading control. Blots were scanned and the signal subsequently quantified using ImageJ software (NIH).

Statistical analysis

Data were analyzed in Prism (GraphPad Software, San Diego, CA) and expressed as mean ± standard deviation. Inter-group comparisons were performed using the two-tailed unpaired Student's t test for normally distributed data, and Mann-Whitney test for non-normally distributed data. The significance level was set at alpha = 0.05. All experiments were performed in at least triplicate with at least three replicates per condition per experiment.

Results

TTFields, similarly to TMZ chemotherapy, reduces [^{18}F]DASA-23 uptake in GBM

The IC_{50} of cell viability due to TMZ in U87 cells was determined to be 484 µM over a 72 h incubation period (Figure 2A, Hill slope −0.9; Log IC_{50} 2.7) which was consistent with previous reports [30,31]. We have previously reported 200 kHz TTFields to be the optimal frequency for impairing GBM cell proliferation [32]; therefore, this frequency was

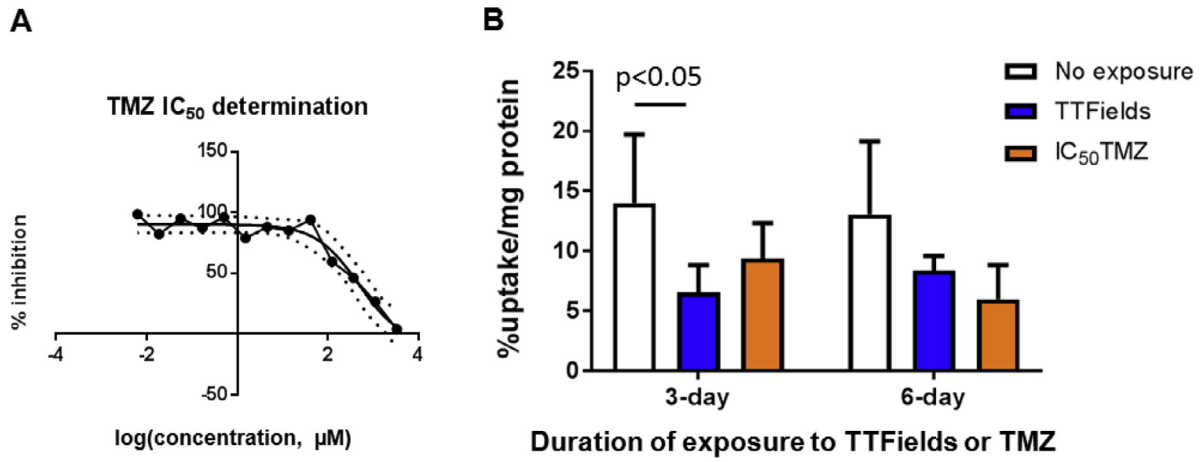

Figure 2. [^{18}F]DASA-23 cellular uptake in U87 cells treated with either temozolomide (TMZ) chemotherapy or TTFields. (A) TMZ IC_{50} of cell viability determination in U87 cells after 72 h of exposure. (B) [^{18}F]DASA-23 cellular uptake over 30 min in U87 cells exposed for 3 or 6 d to the IC_{50} of TMZ, 200 kHz TTFields, or neither ($n = 3$ per condition).

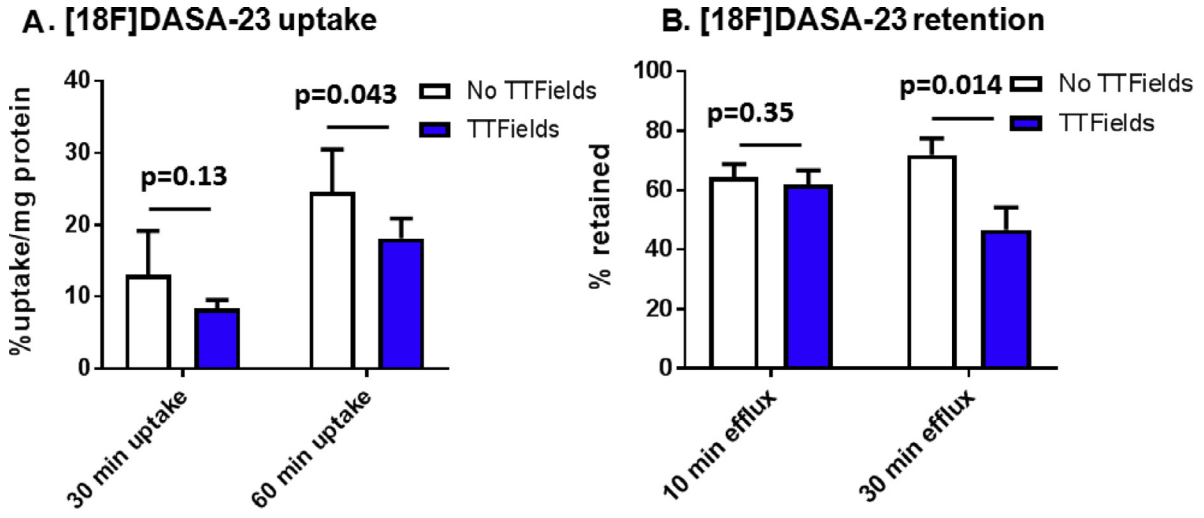

Figure 3. Cellular uptake and retention of [^{18}F]DASA-23 in U87 cells after 6 d of exposure or non-exposure to 200 kHz TTFields. (A) Tumor cell uptake of [^{18}F]DASA-23 over 30- and 60-min periods after 6 d of exposure or non-exposure to TTFields ($n \geq 3$ per condition). (B) Retention of [^{18}F]DASA-23 in U87 cells at 10- and 30-min post-removal of [^{18}F]DASA-23-containing media in U87 cells after 6 d of exposure or non-exposure to 200 kHz TTFields ($n \geq 4$ per condition).

applied for radiotracer uptake studies and will subsequently be referred to as TTFields. U87 cellular uptake studies with [^{18}F]DASA-23 following a 3-d exposure to either TTFields or the IC_{50} of TMZ resulted in a 53% ($P < 0.05$) and 33% reduction in radiotracer uptake relative to untreated cells, respectively (Figure 2B). After a 6-d exposure to either TTFields or the IC_{50} of TMZ, the [^{18}F]DASA-23 uptake in U87 cells was reduced by 35% and 55%, respectively, compared to that in unexposed cells (Figure 2B).

Characterization of [^{18}F]DASA-23 radiotracer uptake and retention in human GBM cells exposed to TTFields

We next characterized the uptake of the [^{18}F]DASA-23 radiotracer in U87 cells unexposed versus exposed to TTFields. U87 cells unexposed to TTFields for 6 d (i.e., normal cell culture conditions) exhibited [^{18}F]DASA-23 radiotracer uptake values of 13.1% ± 6.1% and 24.6% ± 5.9% uptake/mg protein at 30 and 60 min post-addition of radioactivity, respectively (Figure 3A). In contrast, U87 cells exposed to TTFields for 6 d had reduced radiotracer uptake values at 30- and 60-min post-addition of radioactivity, respectively, of 8.4% ± 1.2% uptake/mg protein (35% reduction compared to unexposed cells, $P = 0.13$) and 18.1% ± 2.7% uptake/mg protein (31% reduction compared to unexposed cells, $P = 0.043$), see Figure 3A.

In the retention studies, removal of the [^{18}F]DASA-23 radiotracer from the cell media resulted in variable amounts of efflux of the cell-associated radioactivity. The percentage of [^{18}F]DASA-23 at 10 min post-removal of [^{18}F]DASA-23-containing media was 64.3% ± 4.5% in TTFields-unexposed cells and 62.0% ± 4.7% in TTFields-exposed cells for 6 d ($P = 0.42$, $n = 5$), see Figure 3B. At 30 min post-removal of [^{18}F]DASA-23-containing media, the percentage of radiotracer still retained was 72.0% ± 5.6% in unexposed cells ($P = 0.35$ compared to unexposed cells) but significantly lower at 46.7% ± 7.5% ($P = 0.014$ compared to unexposed cells) in cells exposed to TTFields for 6 d (Figure 3B).

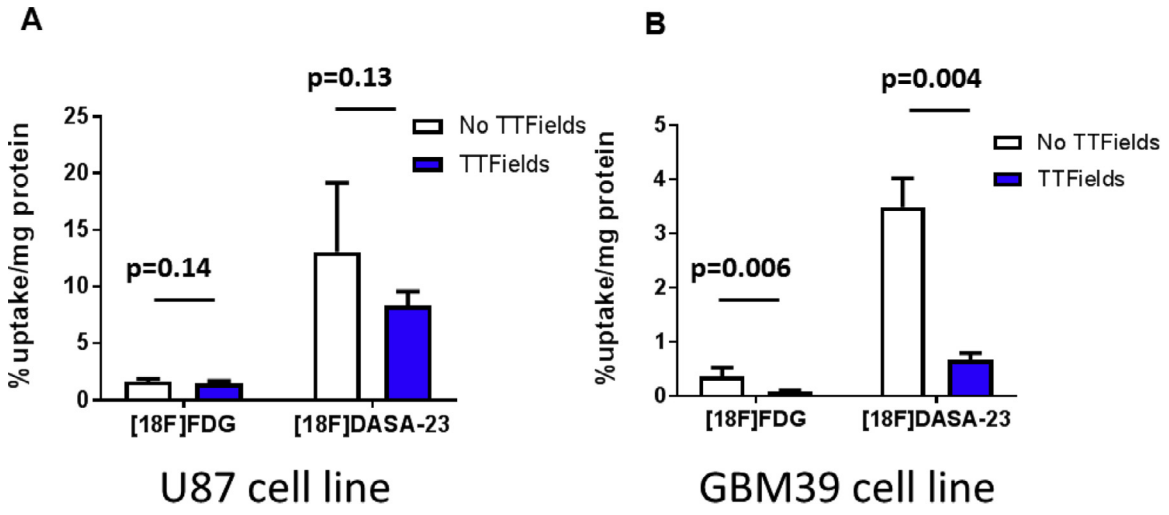

Figure 4. Comparative uptake of [^{18}F]DASA-23 and [^{18}F]FDG in U87 and GBM39 human glioblastoma cells in response to a 6-d exposure to 200 kHz TTFields. (A) Cellular uptake of [^{18}F]DASA-23 and [^{18}F]FDG over 30 min in U87 cells following 6-d TTFields exposure compared to unexposed cells. (B) Cellular uptake of [^{18}F]DASA-23 and [^{18}F]FDG over 30 min in GBM39 cells following 6-d TTFields exposure compared to unexposed cells.

Bigger decrease in uptake of [^{18}F]DASA-23 compared to [^{18}F]FDG in human GBM cells exposed to TTFields

We next compared the ability of [^{18}F]DASA-23 to detect TTFields-induced changes in GBM cell metabolism compared to the established glycolytic radiotracer, [^{18}F]FDG. In U87 cells, a 6-d exposure to TTFields resulted in a 35% reduction of [^{18}F]DASA-23 during the 30-min uptake period compared to unexposed cells ($P = 0.13$) and an 8% reduction (1.5% ± 0.2% vs 1.6% ± 0.2% uptake/mg protein) of [^{18}F]FDG during the 30-min uptake period compared to unexposed cells ($P = 0.14$), see Figure 4A. In patient-derived GBM39 cells, a 6-d exposure to TTFields resulted in a 81% reduction (0.7% ± 0.1% vs 3.5% ± 0.5% uptake/mg protein) of [^{18}F]DASA-23 during the 30-min uptake period compared to unexposed cells ($P = 0.004$) and a 76% reduction (0.09% ± 0.02% vs 0.4% ± 0.2% uptake/mg protein) of [^{18}F]FDG during the 30-min uptake period compared to unexposed cells ($P = 0.006$), see Figure 4B. Although there was a comparable percent reduction in uptake of both radiotracers in response to TTFields exposure in the GBM39 cell line (81% reduction in [^{18}F]DASA-23 uptake and 76% reduction in [^{18}F]FDG uptake), the absolute values of uptake were an order of magnitude greater for [^{18}F]DASA-23 (3.5% ± 0.5% and 0.7% ± 0.1% uptake/mg protein in TTFields unexposed and exposed cells, respectively) compared to [^{18}F]FDG (0.4% ± 0.2% and 0.09% ± 0.02% uptake/mg protein in TTFields unexposed and exposed cells, respectively).

TTFields exposure reduces PKM2 expression in human GBM cells

Exposure of U87 cells to TTFields resulted in significant reduction of PKM2 expression detected by Western blot. Compared to no TTFields exposure, TTFields exposure reduced PKM2 expression by 49% at 3 d ($P = 0.02$) and by 80% at 6 d ($P = 0.008$), see Figure 5.

TTFields exposure reduces PKM2 expression in human GBM cells (continued)

The reduction in PKM2 expression due to TTFields was qualitatively confirmed through immunofluorescence staining for PKM2 and DAPI in U87 and GBM39 cells (Figure 6). In both cell lines, a reduction in cell count after the 6-d TTFields exposure was observed. In addition, there was reduced PKM2 expression in the remaining viable cells after TTFields exposure compared to cells that were not exposed to TTFields.

Discussion

In the past decade, antimitotic frequency-tuned alternating electric fields, known as TTFields, have been validated in clinical trials and represent a novel form of cancer therapy. TTFields are low-intensity (1 to 4 V/cm) intermediate frequency (50 to 500 kHz) alternating electric fields that locally target solid organ cancer through transducer arrays applied on the skin. Despite the clinical survival benefit demonstrated with the combination of TTFields and chemotherapy in GBM [6,7] and malignant pleural mesothelioma [33], the imaging modalities used to track treatment response (e.g., brain MRI scans and chest CT scans, respectively) are not able to capture changes in the tumor based on anatomy alone. This may be due in part to the limited understanding of the mechanisms of action of TTFields beyond their effect on mitosis in cancer cells. Molecular imaging modalities such as PET play a prominent role in cancer imaging [15], but due to its low tumor-to-background ratio in the brain, the most commonly used clinical radiotracer ([^{18}F]FDG) has limited utility in brain tumor imaging [16].

Aside from their elevated rates of proliferation, cancer cells commonly demonstrate aberrant metabolism that is defined by an overutilization of glycolysis relative to oxidative phosphorylation. This altered metabolic state, often termed metabolic reprogramming, is a hallmark of cancer and is closely linked to the proliferative state of the tumor [34-36]. The clinical implications of tumor metabolic reprogramming are that therapeutic strategies, which revert this metabolism towards oxidative phosphorylation (whether directly or indirectly), may reduce the tumor growth rate and be predictive of survival outcomes [37-39]. PKM2 was identified as an attractive target for measuring aberrant GBM metabolism due to its overexpression in GBM and minimal expression in healthy brain tissue [22]. Additionally, we have recently developed an FDA-approved radiotracer, [^{18}F]DASA-23, for the molecular imaging of PKM2. This radiotracer has been shown to be safe in humans [40] and identifies changes in GBM aberrant glycolysis in response to various drugs used in the clinic [41].

In this study, we report the evaluation of TTFields on aberrant GBM glycolysis and explore the utility of [^{18}F]DASA-23 to detect these shifts in glycolysis through measurement of PKM2. Continuous TTFields exposure in

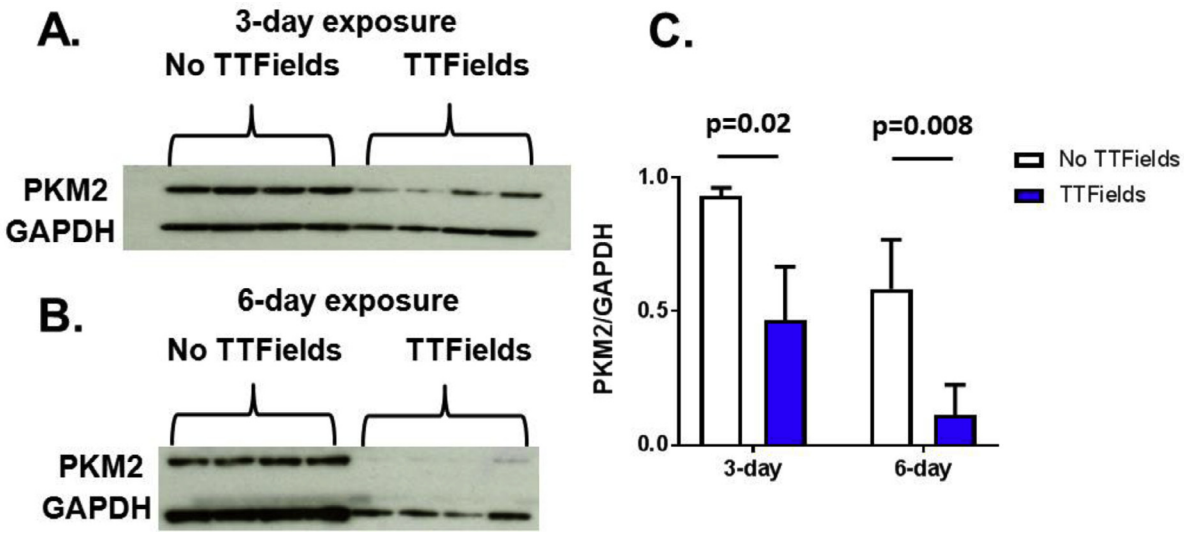

Figure 5. Reduction in pyruvate kinase M2 (PKM2) protein expression in U87 cells exposed for 3- and 6 d to 200 kHz TTFields. (A) Western blot evaluating changes in PKM2 expression after 3 d of TTFields exposure compared to unexposed cells. (B) Western blot evaluating changes in PKM2 expression after 6 d of TTFields exposure compared to unexposed cells. (C) Quantification of Western blot data and normalization using GAPDH as the loading control.

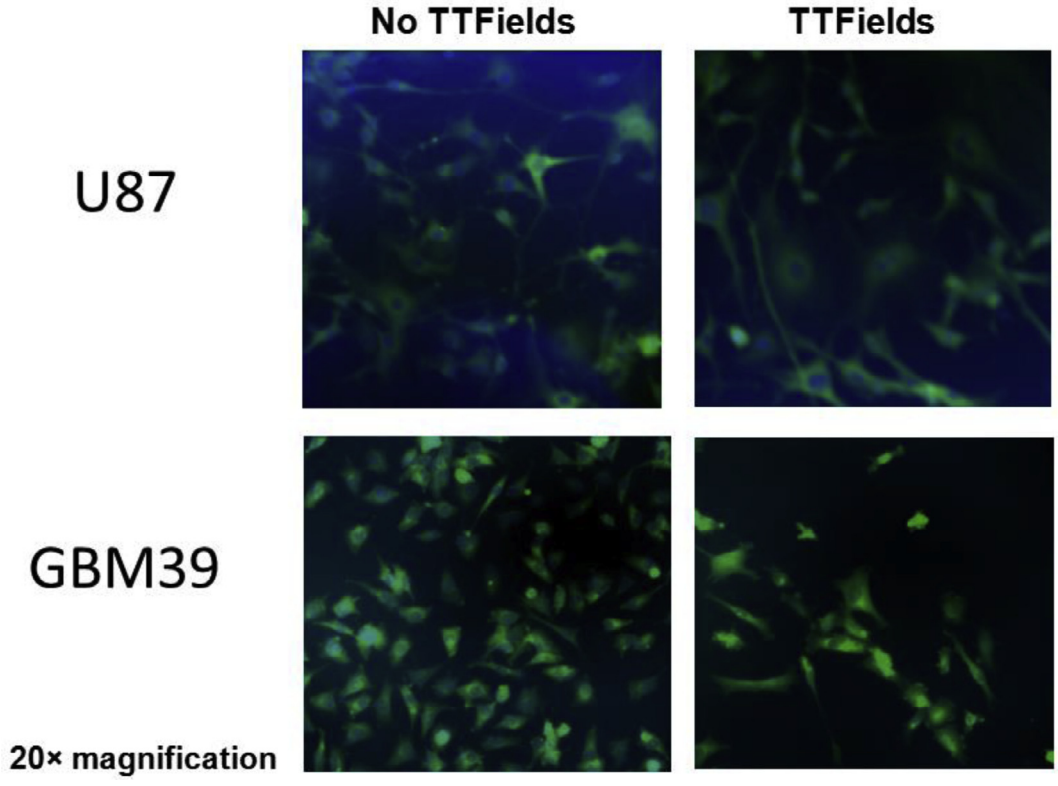

Figure 6. Representative immunofluorescence for PKM2 (green) and DAPI nuclear stain (blue) in U87 and GBM39 cells exposed or unexposed to 200 kHz TTFields for 6 d, demonstrating a reduction in cell count and PKM2 expression after TTFields exposure.

cell culture is similar to the clinically recommended 75% daily compliance for patients with GBM [6,7]. [^{18}F]DASA-23 is a PKM2 activator, known to bind a pocket present at the dimeric PKM2 subunit interface thereby promoting association of PKM2 subunits into stable tetramers [20]. [^{18}F]DASA-23 can bind dimeric PKM2 and promote the association into active tetramers; however, the binding pocket for [^{18}F]DASA-23 is unavailable on constituently active tetramers due to the conformational change associated with tetramer formation [20]. Therefore, reduced [^{18}F]DASA-23 binding in GBMs exposed to TTFields may be associated with 2 factors: (1) reduced PKM2 expression and (2) activation of PKM2 dimers to tetramers. The inability of [^{18}F]DASA-23 to distinguish between these two features is a limitation of this approach. Regardless, both outcomes suggest a shift from aberrant glycolysis towards oxidative phosphorylation [20,42-44].

The application of TTFields in U87 cells for 3- or 6 d resulted in a decrease in [^{18}F]DASA-23 radiotracer uptake that was statistically significant only for the 3-d TTFields exposure condition (Figure 2B). Compared to the results in Figure 2B (which show a significant reduction in 30-min [^{18}F]DASA-23 radiotracer uptake after a 3-d exposure to TTFields), the results in Figure 3A demonstrate a significant reduction in 60-min [^{18}F]DASA-23 radiotracer uptake after a 6-d exposure to TTFields. From a clinical translation perspective, this suggests that the optimal acquisition of PET scans to interrogate GBM metabolic changes in patients before versus after chronic TTFields therapy may be approximately 60-min post-injection of the [^{18}F]DASA-23 radiotracer. In the case of patient-derived GBM39 cells, a 6-d treatment with TTFields was selected based on the slightly slower rate of cell doubling (2 d in U87 vs 3 d in GBM39). In this setting, [^{18}F]DASA-23 radiotracer uptake was significantly reduced (Figure 4B). Although there were reductions in [^{18}F]FDG and [^{18}F]DASA-23 uptake in the U87 and GBM39 cell lines, statistical significance was only achieved in the GBM 39 cell line. This is likely a reflection of inherent differences between different human GBM cell lines (e.g., variable baseline PKM2 expression levels, doubling times, and maintenance culture conditions [32]). The reduced expression of PKM2 protein levels in response to TTFields was confirmed in both U87 and GBM39 cells using a combination of Western blot (Figure 5) and immunofluorescence (Figure 6) techniques, suggesting that the reduction in [^{18}F]DASA-23 cellular uptake may be the result of reduced PKM2 expression rather than changes in enzymatic state. The use of glyceraldehyde 3-phosphate dehydrogenase (GAPDH) as a loading control was selected based on the knowledge that TTFields has known effects on microtubules [45] and actin [46] therefore limiting the use of α-tubulin and β-actin as loading controls. Although the effects of TTFields on GAPDH expression are unknown, it was selected due to its established use as a loading control in human glioma studies [47] and the limited availability of other suitable loading controls. We have previously shown in U87 cells treated with 11 different GBM therapeutic drugs that there is a positive correlation between the normalized [^{18}F]DASA-23 cellular uptake and the normalized PKM2/GAPDH ratio from Western blot analysis [41]. Although a positive correlation exists between the ability of these two methods ([^{18}F]DASA-23 radiotracer uptake and a gold-standard [e.g., Western blot]) to detect changes in PKM2 expression, the inherent differences in the sensitivity and specificity of each method precludes a consistent one-to-one concordance between the statistical significance results derived from each method, as demonstrated in Figsure 4 and 5.

To further elucidate a shift towards oxidative metabolism in response to a 6-d TTFields exposure, the cellular uptake of [^{18}F]FDG was also evaluated in U87 and GBM39 cells relative to control cells. Although [^{18}F]DASA-23 and [^{18}F]FDG exhibited decreased uptake in human GBM cells exposed to TTFields (Figure 4), [^{18}F]DASA-23 likely holds greater clinical utility for brain tumor molecular imaging due to the overexpression of PKM2 in GBM cells and a lack of PKM2 expression in healthy brain tissue, as well as its 10-fold greater absolute radiotracer uptake values compared to those of [^{18}F]FDG. The % uptake/mg protein values from cell culture studies are analogous to the standardized uptake values determined on in vivo PET scans. Given that [^{18}F]DASA-23 uptake in the human GBM cell lines was 10-fold greater than that of [^{18}F]FDG, and there is less [^{18}F]DASA-23 compared to [^{18}F]FDG uptake in the normal brain, we would anticipate [^{18}F]DASA-23 could better detect and monitor GBM metabolic response to therapy compared to [^{18}F]FDG. [^{18}F]DASA-23 is additionally approved by the FDA for evaluation in human subjects [40], further highlighting the clinical translatability of this approach. Importantly, the [^{18}F]DASA-23 retention studies after an initial 30-min uptake period (Figure 3B) demonstrated a net efflux of [^{18}F]DASA-23 out of the cell from 10- to 30 min under TTFields exposure, while there was a slight net influx without TTFields exposure during the same period. This is consistent with our previous finding that TTFields causes fenestrations in the GBM cell membranes, thereby increasing the cell membrane permeability [10].

The role of adenosine triphosphate (ATP) in cancer is multifactorial, and its generation via glycolysis versus oxidative phosphorylation varies under different conditions and cancer cell types [48-50]. For example, one study reported that TTFields reduced intracellular ATP levels in an autophagy-dependent manner in a human lung carcinoma cell line [51]. Another group found that human pancreatic ductal cell carcinoma cells can rely on mitochondrial oxidative phosphorylation for ATP generation and survival when glycolysis is suppressed [52]. The standard therapies used to treat GBM (e.g., radiation therapy and TMZ chemotherapy) may themselves cause a metabolic reprogramming rendering the GBM cells more resistant to therapy [53]. Our finding that TTFields inhibits aberrant glycolysis may help to explain how GBM cells overcome an inherent resistance to standard therapies, thereby prolonging patient survival [6,7].

While these results are encouraging and suggest the potential for early response assessment to TTFields using PET imaging of PKM2 expression with [^{18}F]DASA-23, there are several limitations of the present work. First, there is no currently available apparatus for delivering TTFields to the mouse brain, which limited our experiments to human GBM cell lines in culture. However, it should be noted that despite the U87 cells having non-methylation of the promoter of the O^6-methylguanine-DNA-methyltransferase (MGMT) DNA repair enzyme and the GBM39 cells having MGMT promoter methylation, indicating a differential responsiveness to TMZ chemotherapy [54], both cells demonstrated reduced [^{18}F]DASA23 uptake and PKM2 expression in response to TTFields. Likewise, an overall survival benefit was observed in GBM patients treated with TTFields in combination with adjuvant TMZ, regardless of MGMT promoter methylation status [6]. Second, the present studies have not elucidated the mechanism through which TTFields affects aberrant GBM glycolysis and whether the detected shift in metabolism is the result of a direct effect of TTFields on a specific protein, or the result of a bystander effect. It should be noted that this is beyond the scope of the present manuscript which is a proof of principle study.

Amino acid-based PET [11,12] and perfusion/spectroscopic MRI [13] have demonstrated changes in human GBM after months of TTFields therapy, but an imaging biomarker of early response assessment to TTFields is lacking in the field of neuro-oncology. If validated in an ongoing clinical trial (NCT03539731), [^{18}F]DASA23 PET has the potential to provide an early non-invasive readout of GBM response to TTFields therapy.

Conclusions

This is the first study to demonstrate that TTFields causes a shift in GBM metabolism from glycolysis to oxidative phosphorylation. Furthermore, these changes can be detected non-invasively with the [^{18}F]DASA-23 radiotracer that is specific for pyruvate kinase M2, which catalyzes the last step in tumor glycolysis. These findings are being translated to determine whether [^{18}F]DASA-23 can detect response to TTFields in patients with GBM.

Prior publication

This work was previously presented in abstract form at the 2018 Society for Neuro-Oncology Meeting, 2018 World Molecular Imaging Congress, and 2019 American Association for Cancer Research Meeting.

CRediT authorship contribution statement

Chirag B. Patel: Conceptualization, Formal analysis, Funding acquisition, Investigation, Methodology, Project administration, Writing - original draft, Writing - review & editing. **Corinne Beinat:** Conceptualization, Formal analysis, Investigation, Methodology, Writing

- original draft, Writing - review & editing. **Yuanyang Xie:** Investigation, Methodology, Writing - review & editing. **Edwin Chang:** Methodology, Writing - review & editing. **Sanjiv S. Gambhir:** Conceptualization, Funding acquisition, Writing - review & editing.

Acknowledgments

We thank the Radiochemistry Facility at Stanford University for the ^{18}F production, in particular Drs. Bin Shen, Jun Hyung Park, and Jessa B. Castillo. We thank George Montoya for the [^{18}F]FDG production.

References

[1] Killock D. CNS cancer: TTFields improve survival. *Nat Rev Clin Oncol* 2018;**15**:136 Epub 2018 Jan 16. PMID: 29335650. doi:10.1038/nrclinonc.2018.2.

[2] Mun EJ, Babiker HM, Weinberg U, Kirson ED, Von Hoff DD. Tumor-treating fields: a fourth modality in cancer treatment. *Clin Cancer Res* 2018;**24**:266–75 Epub 2017 Aug 1. PMID: 28765323. doi:10.1158/1078-0432.CCR-17-1117.

[3] Rick J, Chandra A, Aghi MK. Tumor treating fields: a new approach to glioblastoma therapy. *J Neurooncol* 2018;**137**:447–53 Epub 2018 Jan 18. PMID: 29349613. doi:10.1007/s11060-018-2768-x.

[4] Zhang I, Knisely JP. Tumor-treating fields-a fundamental change in locoregional management for glioblastoma. *JAMA Oncol* 2016;**2**:813–14 PMID: 26986446. doi:10.1001/jamaoncol.2016.0081.

[5] Lok E, Swanson KD, Wong ET. Tumor treating fields therapy device for glioblastoma: physics and clinical practice considerations. *Expert Rev Med Devices* 2015;**12**:717–26 Epub 2015 Oct 29. PMID: 26513694. doi:10.1586/17434440.2015.1086641.

[6] Stupp R, Taillibert S, Kanner A, Read W, Steinberg D, Lhermitte B, Toms S, Idbaih A, Ahluwalia MS, Fink K, et al. Effect of tumor-treating fields plus maintenance temozolomide vs maintenance temozolomide alone on survival in patients with glioblastoma: a randomized clinical trial. *JAMA* 2017;**318**:2306–16 Erratum in: JAMA. 2018 May 1;319(17):1824. PMID: 29260225; PMCID: PMC5820703. doi:10.1001/jama.2017.18718.

[7] Stupp R, Taillibert S, Kanner AA, Kesari S, Steinberg DM, Toms SA, Taylor LP, Lieberman F, Silvani A, Fink KL, et al. Maintenance therapy with tumor-treating fields plus temozolomide vs temozolomide alone for glioblastoma: a randomized clinical trial. *JAMA* 2015;**314**:2535–43 PMID: 26670971. doi:10.1001/jama.2015.16669.

[8] Giladi M, Schneiderman RS, Voloshin T, Porat Y, Munster M, Blat R, Sherbo S, Bomzon Z, Urman N, Itzhaki A, et al. Mitotic spindle disruption by alternating electric fields leads to improper chromosome segregation and mitotic catastrophe in cancer cells. *Sci Rep* 2015;**5**:18046 PMID: 26658786; PMCID: PMC4676010. doi:10.1038/srep18046.

[9] Gera N, Yang A, Holtzman TS, Lee SX, Wong ET, Swanson KD. Tumor treating fields perturb the localization of septins and cause aberrant mitotic exit. *PLoS One* 2015;**10**:e0125269 PMID: 26010837; PMCID: PMC4444126. doi:10.1371/journal.pone.0125269.

[10] Chang E, Patel CB, Pohling C, Young C, Song J, Flores TA, Zeng Y, Joubert LM, Arami H, Natarajan A, et al. Tumor treating fields increases membrane permeability in glioblastoma cells. *Cell Death Discov* 2018;**4**:113 PMID: 30534421; PMCID: PMC6281619. doi:10.1038/s41420-018-0130-x.

[11] Bosnyák E, Barger GR, Michelhaugh SK, Robinette NL, Amit-Yousif A, Mittal S, Juhász C. Amino acid PET imaging of the early metabolic response during tumor-treating fields (TTFields) therapy in recurrent glioblastoma. *Clin Nucl Med* 2018;**43**:176–9 PMID: 29261637; PMCID: PMC6816242. doi:10.1097/RLU.0000000000001942.

[12] Ceccon G, Lazaridis L, Stoffels G, Rapp M, Weber M, Blau T, Lohmann P, Kebir S, Herrmann K, Fink GR, et al. Use of FET PET in glioblastoma patients undergoing neurooncological treatment including tumour-treating fields: initial experience. *Eur J Nucl Med Mol Imaging* 2018;**45**:1626–35 Epub 2018 Mar 21. PMID: 29564490. doi:10.1007/s00259-018-3992-5.

[13] Mohan S, Chawla S, Wang S, Verma G, Skolnik A, Brem S, Peters KB, Poptani H. Assessment of early response to tumor-treating fields in newly diagnosed glioblastoma using physiologic and metabolic MRI: initial experience. *CNS Oncol* 2016;**5**:137–44 Epub 2016 Apr 14. PMID: 27076281; PMCID: PMC6042635. doi:10.2217/cns-2016-0003.

[14] Warburg O. On the origin of cancer cells. *Science* 1956;**123**:309–14 PMID: 13298683. doi:10.1126/science.123.3191.309.

[15] Kelloff GJ, Hoffman JM, Johnson B, Scher HI, Siegel BA, Cheng EY, Cheson BD, O'shaughnessy J, Guyton KZ, Mankoff DA, et al. Progress and promise of FDG-PET imaging for cancer patient management and oncologic drug development. *Clin Cancer Res* 2005;**11**:2785–808 PMID: 15837727. doi:10.1158/1078-0432.CCR-04-2626.

[16] Albert NL, Weller M, Suchorska B, Galldiks N, Soffietti R, Kim MM, la Fougère C, Pope W, Law I, Arbizu J, et al. Response Assessment in Neuro-Oncology working group and European Association for Neuro-Oncology recommendations for the clinical use of PET imaging in gliomas. *Neuro Oncol* 2016;**18**:1199–208 Epub 2016 Apr 21. PMID: 27106405; PMCID: PMC4999003. doi:10.1093/neuonc/now058.

[17] Beinat C, Alam IS, James ML, Srinivasan A, Gambhir SS. Development of [^{18}F]DASA-23 for imaging tumor glycolysis through noninvasive measurement of pyruvate kinase M2. *Mol Imaging Biol* 2017;**19**:665–72 PMID: 28236227. doi:10.1007/s11307-017-1068-8.

[18] Wong N, De Melo J, Tang D. PKM2, a central point of regulation in cancer metabolism. *Int J Cell Biol* 2013;**2013**:242513 Epub 2013 Feb 14. PMID: 23476652; PMCID: PMC3586519. doi:10.1155/2013/242513.

[19] Agnihotri S, Zadeh G. Metabolic reprogramming in glioblastoma: the influence of cancer metabolism on epigenetics and unanswered questions. *Neuro Oncol* 2016;**18**:160–72 Epub 2015 Jul 14. PMID: 26180081; PMCID: PMC4724176. doi:10.1093/neuonc/nov125.

[20] Anastasiou D, Yu Y, Israelsen WJ, Jiang JK, Boxer MB, Hong BS, Tempel W, Dimov S, Shen M, Jha A, et al. Pyruvate kinase M2 activators promote tetramer formation and suppress tumorigenesis. *Nat Chem Biol* 2012;**8**:839–47 Erratum in: Nat Chem Biol. 2012 Dec;8(12):1008. PMID: 22922757; PMCID: PMC3711671. doi:10.1038/nchembio.1060.

[21] Zhu H, Luo H, Zhu X, Hu X, Zheng L, Zhu X. Pyruvate kinase M2 (PKM2) expression correlates with prognosis in solid cancers: a meta-analysis. *Oncotarget* 2017;**8**:1628–40 PMID: 27911861; PMCID: PMC5352083. doi:10.18632/oncotarget.13703.

[22] Mukherjee J, Phillips JJ, Zheng S, Wiencke J, Ronen SM, Pieper RO. Pyruvate kinase M2 expression, but not pyruvate kinase activity, is up-regulated in a grade-specific manner in human glioma. *PLoS One* 2013;**8**:e57610 Epub 2013 Feb 25. PMID: 23451252; PMCID: PMC3581484. doi:10.1371/journal.pone.0057610.

[23] Christofk HR, Vander Heiden MG, Harris MH, Ramanathan A, Gerszten RE, Wei R, Fleming MD, Schreiber SL, Cantley LC. The M2 splice isoform of pyruvate kinase is important for cancer metabolism and tumour growth. *Nature* 2008;**452**:230–3 PMID: 18337823. doi:10.1038/nature06734.

[24] Giladi M, Munster M, Schneiderman RS, Voloshin T, Porat Y, Blat R, Zielinska-Chomej K, Hååg P, Bomzon Z, Kirson ED, et al. Tumor treating fields (TTFields) delay DNA damage repair following radiation treatment of glioma cells. *Radiat Oncol* 2017;**12**:206 PMID: 29284495; PMCID: PMC5747183. doi:10.1186/s13014-017-0941-6.

[25] Giladi M, Schneiderman RS, Porat Y, Munster M, Itzhaki A, Mordechovich D, Cahal S, Kirson ED, Weinberg U, Palti Y. Mitotic disruption and reduced clonogenicity of pancreatic cancer cells in vitro and in vivo by tumor treating fields. *Pancreatology* 2014;**14**:54–63 Epub 2013 Dec 4. PMID: 24555979. doi:10.1016/j.pan.2013.11.009.

[26] Karanam NK, Srinivasan K, Ding L, Sishc B, Saha D, Story MD. Tumor-treating fields elicit a conditional vulnerability to ionizing radiation via the downregulation of BRCA1 signaling and reduced DNA double-strand break repair capacity in non-small cell lung cancer cell lines. *Cell Death Dis* 2017;**8**:e2711 PMID: 28358361; PMCID: PMC5386539. doi:10.1038/cddis.2017.136.

[27] Kirson ED, Dbalý V, Tovarys F, Vymazal J, Soustiel JF, Itzhaki A, Mordechovich D, Steinberg-Shapira S, Gurvich Z, Schneiderman R, et al. Alternating electric fields arrest cell proliferation in animal tumor models and human brain tumors. *Proc Natl Acad Sci U S A* 2007;**104**:10152–7 Epub

2007 Jun 5. PMID: 17551011; PMCID: PMC1886002. doi:10.1073/pnas.0702916104.

[28] Schneiderman RS, Shmueli E, Kirson ED, Palti Y. TTFields alone and in combination with chemotherapeutic agents effectively reduce the viability of MDR cell sub-lines that over-express ABC transporters. *BMC Cancer* 2010;**10**:229 PMID: 20492723; PMCID: PMC2893108. doi:10.1186/1471-2407-10-229.

[29] Kim EH, Song HS, Yoo SH, Yoon M. Tumor treating fields inhibit glioblastoma cell migration, invasion and angiogenesis. *Oncotarget* 2016;**7**:65125–36 PMID: 27556184; PMCID: PMC5323142. doi:10.18632/oncotarget.11372.

[30] Perazzoli G, Prados J, Ortiz R, Caba O, Cabeza L, Berdasco M, Gónzalez B, Melguizo C. Temozolomide resistance in glioblastoma cell lines: implication of MGMT, MMR, P-Glycoprotein and CD133 Expression. *PLoS One* 2015;**10**:e0140131 PMID: 26447477; PMCID: PMC4598115. doi:10.1371/journal.pone.0140131.

[31] Castro GN, Cayado-Gutiérrez N, Zoppino FC, Fanelli MA, Cuello-Carrión FD, Sottile M, Nadin SB, Ciocca DR. Effects of temozolomide (TMZ) on the expression and interaction of heat shock proteins (HSPs) and DNA repair proteins in human malignant glioma cells. *Cell Stress Chaperones* 2015;**20**:253–65 Epub 2014 Aug 26. PMID: 25155585; PMCID: PMC4326375. doi:10.1007/s12192-014-0537-0.

[32] Chang E, Pohling C, Beygui N, Patel CB, Rosenberg J, Ha DH, Gambhir SS. Synergistic inhibition of glioma cell proliferation by Withaferin A and tumor treating fields. *J Neurooncol* 2017;**134**:259–68 Epub 2017 Jul 5. PMID: 28681243; PMCID: PMC5711586. doi:10.1007/s11060-017-2534-5.

[33] Ceresoli GL, Aerts JG, Dziadziuszko R, Ramlau R, Cedres S, van Meerbeeck JP, Mencoboni M, Planchard D, Chella A, Crinò L, et al. Tumour Treating Fields in combination with pemetrexed and cisplatin or carboplatin as first-line treatment for unresectable malignant pleural mesothelioma (STELLAR): a multicentre, single-arm phase 2 trial. *Lancet Oncol* 2019;**20**:1702–9 Epub 2019 Oct 15. Erratum in: Lancet Oncol. 2020 Feb;21(2):e70. PubMed PMID: 31628016. doi:10.1016/S1470-2045(19)30532-7.

[34] Ward PS, Thompson CB. Metabolic reprogramming: a cancer hallmark even warburg did not anticipate. *Cancer Cell* 2012;**21**:297–308 PMID: 22439925; PMCID: PMC3311998. doi:10.1016/j.ccr.2012.02.014.

[35] Faubert B, Solmonson A, DeBerardinis RJ. Metabolic reprogramming and cancer progression. *Science* 2020;**368**:eaaw5473 PMID: 32273439. doi:10.1126/science.aaw5473.

[36] DeBerardinis RJ, Lum JJ, Hatzivassiliou G, Thompson CB. The biology of cancer: metabolic reprogramming fuels cell growth and proliferation. *Cell Metab* 2008;**7**:11–20 PMID: 18177721. doi:10.1016/j.cmet.2007.10.002.

[37] Radoul M, Chaumeil MM, Eriksson P, Wang AS, Phillips JJ, Ronen SM. MR studies of glioblastoma models treated with dual PI3K/mTOR inhibitor and temozolomide: metabolic changes are associated with enhanced survival. *Mol Cancer Ther* 2016;**15**:1113–22 Epub 2016 Feb 16. PMID: 26883274; PMCID: PMC4873419. doi:10.1158/1535-7163.MCT-15-0769.

[38] Park I, Mukherjee J, Ito M, Chaumeil MM, Jalbert LE, Gaensler K, Ronen SM, Nelson SJ, Pieper RO. Changes in pyruvate metabolism detected by magnetic resonance imaging are linked to DNA damage and serve as a sensor of temozolomide response in glioblastoma cells. *Cancer Res* 2014;**74**:7115–24 Epub 2014 Oct 15. PMID: 25320009; PMCID: PMC4253720. doi:10.1158/0008-5472.CAN-14-0849.

[39] Rozental JM, Cohen JD, Mehta MP, Levine RL, Hanson JM, Nickles RJ. Acute changes in glucose uptake after treatment: the effects of carmustine (BCNU) on human glioblastoma multiforme. *J Neurooncol* 1993;**15**:57–66 PMID: 8384254. doi:10.1007/BF01050264.

[40] Beinat C, Patel CB, Haywood T, Shen B, Naya L, Gandhi H, Holley D, Khalighi M, Iagaru A, Davidzon G, et al. Human biodistribution and radiation dosimetry of [^{18}F]DASA-23, a PET probe targeting pyruvate kinase M2. *Eur J Nucl Med Mol Imaging* 2020 Epub ahead of print. PMID: 31938892. doi:10.1007/s00259-020-04687-0.

[41] Beinat C, Patel CB, Xie Y, Gambhir SS. Evaluation of glycolytic response to multiple classes of anti-glioblastoma drugs by noninvasive measurement of pyruvate kinase M2 using [^{18}F]DASA-23. *Mol Imaging Biol* 2020;**22**:124–33 PMID: 30989436. doi:10.1007/s11307-019-01353-2.

[42] Gui DY, Lewis CA, Vander Heiden MG. Allosteric regulation of PKM2 allows cellular adaptation to different physiological states. *Sci Signal* 2013;**6**:pe7 PMID: 23423437. doi:10.1126/scisignal.2003925.

[43] Dayton TL, Gocheva V, Miller KM, Bhutkar A, Lewis CA, Bronson RT, Vander Heiden MG, Jacks T. Isoform-specific deletion of PKM2 constrains tumor initiation in a mouse model of soft tissue sarcoma. *Cancer Metab* 2018;**6**:6 PMID: 29854399; PMCID: PMC5977456. doi:10.1186/s40170-018-0179-2.

[44] Hsu MC, Hung WC. Pyruvate kinase M2 fuels multiple aspects of cancer cells: from cellular metabolism, transcriptional regulation to extracellular signaling. *Mol Cancer* 2018;**17**:35 PMID: 29455645; PMCID: PMC5817853. doi:10.1186/s12943-018-0791-3.

[45] Kirson ED, Gurvich Z, Schneiderman R, Dekel E, Itzhaki A, Wasserman Y, Schatzberger R, Palti Y. Disruption of cancer cell replication by alternating electric fields. *Cancer Res* 2004;**64**:3288–95 PMID: 15126372. doi:10.1158/0008-5472.can-04-0083.

[46] Schneiderman R, Zeevi E, Voloshin T, Shteingauz A, Giladi M, Porat Y, Munster M, Kirson ED, Weinberg U, Palti Y. CBIO-30 tumor treating fields (TTFields) inhibit cancer cell migration and invasion by inducing reorganization of the actin cytoskeleton and formation of cell adhesions. *Neuro-Oncology* 2017;**19**(Suppl 6):vi38 Epub 2017 Nov 6. PMCID: PMC5692971. doi:10.1093/neuonc/nox168.148.

[47] Kreth S, Heyn J, Grau S, Kretzschmar HA, Egensperger R, Kreth FW. Identification of valid endogenous control genes for determining gene expression in human glioma. *Neuro Oncol* 2010;**12**:570–9 Epub 2010 Feb 5. PMID: 20511187; PMCID: PMC2940642. doi:10.1093/neuonc/nop072.

[48] Israelsen WJ, Vander Heiden MG. ATP consumption promotes cancer metabolism. *Cell* 2010;**143**:669–71 PMID: 21111226. doi:10.1016/j.cell.2010.11.010.

[49] Vander Heiden MG, DeBerardinis RJ. Understanding the Intersections between metabolism and cancer biology. *Cell* 2017;**168**:657–69 PMID: 28187287; PMCID: PMC5329766. doi:10.1016/j.cell.2016.12.039.

[50] Strickland M, Stoll EA. Metabolic reprogramming in glioma. *Front Cell Dev Biol* 2017;**5**:43 PMID: 28491867; PMCID: PMC5405080. doi:10.3389/fcell.2017.00043.

[51] Voloshin T, Kaynan N, Davidi S, Porat Y, Shteingauz A, Schneiderman RS, Zeevi E, Munster M, Blat R, Tempel Brami C, Cahal S, et al. Tumor-treating fields (TTFields) induce immunogenic cell death resulting in enhanced antitumor efficacy when combined with anti-PD-1 therapy. *Cancer Immunol Immunother* 2020;**69**:1191–204 Epub 2020 Mar 6. PMID: 32144446; PMCID: PMC7303058. doi:10.1007/s00262-020-02534-7.

[52] Shiratori R, Furuichi K, Yamaguchi M, Miyazaki N, Aoki H, Chibana H, Ito K, Aoki S. Glycolytic suppression dramatically changes the intracellular metabolic profile of multiple cancer cell lines in a mitochondrial metabolism-dependent manner. *Sci Rep* 2019;**9**:18699 PMID: 31822748; PMCID: PMC6904735. doi:10.1038/s41598-019-55296-3.

[53] Seyfried TN, Flores R, Poff AM, D'Agostino DP, Mukherjee P. Metabolic therapy: a new paradigm for managing malignant brain cancer. *Cancer Lett* 2015;**356**(2 Pt A):289–300 Epub 2014 Jul 25. PMID: 25069036. doi:10.1016/j.canlet.2014.07.015.

[54] Hegi ME, Diserens AC, Gorlia T, Hamou MF, de Tribolet N, Weller M, Kros JM, Hainfellner JA, Mason W, Mariani L, et al. MGMT gene silencing and benefit from temozolomide in glioblastoma. *N Engl J Med* 2005;**352**:997–1003 PMID: 15758010. doi:10.1056/NEJMoa043331.